

Supporting Information

Control of higher-order structures of zinc chlorophyll
coordination polymers

Yoshinao Shinozaki,^a Isao Yoshikawa,^b Koji Araki,^b Kosuke Sugawa,^a
and Joe Otsuki *^a

^a*College of Science and Technology, Nihon University, 1-18-14, Kanda-Surugadai,
Chiyoda-ku, Tokyo 101-8308*

^b*Institute of Industrial Science, University of Tokyo, 4-6-1, Komaba, Meguro-ku,
Tokyo 153-8505*

Contents

1. Materials and Methods
2. Syntheses and Characterization Data
3. Comparison of ¹H-NMR Spectra for the Free-Base Derivatives and
Their Zinc Complexes
4. Crystallographic Data
5. Relative Efficiency of Förster-type Energy Transfer
6. Fluorescence Spectra

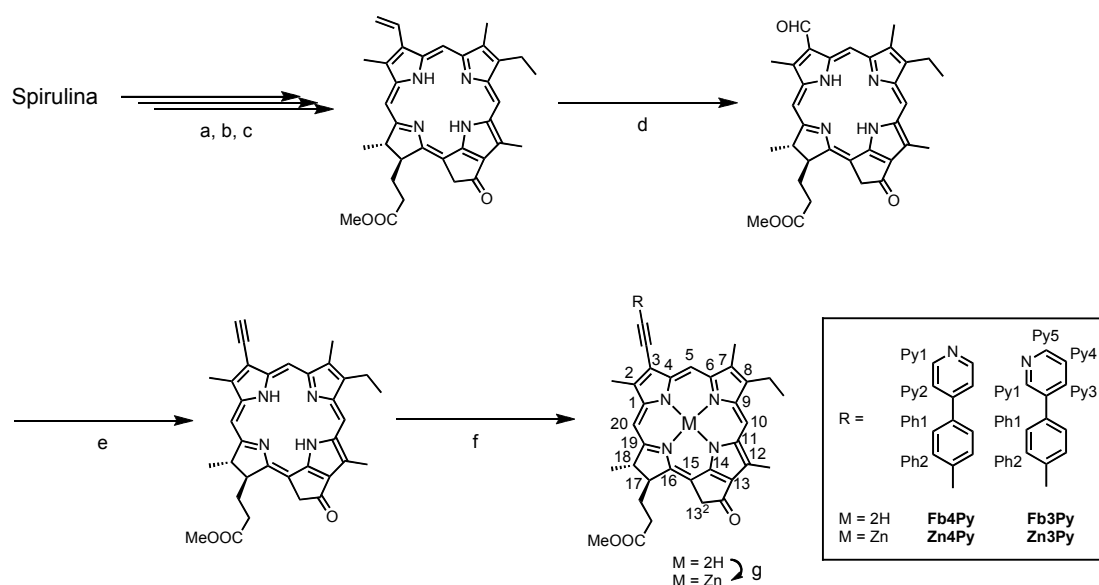
1. Materials and Methods

All reactions were conducted under Ar. All reagents and solvents purchased for syntheses were used without further purification. CDCl_3 was purchased from Sigma-Aldrich.

^1H NMR spectra were recorded with a 400 MHz JEOL ECX 400 spectrometer, and chemical shifts were reported in ppm relative to internal tetramethylsilane (TMS). The peaks were assigned with the help of COSY, NOESY, HMQC, HMBC, and DEPT. Gel permeation chromatography was performed with Japan Analytical Industry LC-9201 equipped with Jaigel-1H and Jaigel-2H columns. High-resolution mass spectrometry analyses were performed with an Agilent G1969A mass spectrometer using positive atmospheric chemical ionization (APCI). The fluorescence spectra were recorded with a JASCO FP-8600 fluorometer. The single crystal diffraction analysis data were collected at 93 K with a Rigaku VariMax Dual with Saturn diffractometer using $\text{Mo K}\alpha$ radiation (0.71075 Å). The structures were solved by direct method using SIR2004¹ for Zn3Py or SIR2011² for Zn4Py, and refined by the full-matrix least-squares method using SHELXL-97.³ Contributions of disordered solvents on the reflection data were removed by the SQUEEZE command in the program PLATON.⁴

1. M. C. Burla, R. Caliendo, M. Camalli, B. Carrozzini, G. L. Cascarano, L. De Caro, C. Giacovazzo, G. Polidori, R. Spagna, *J. Appl. Cryst.* **2005**, *38*, 381-388.
2. M. C. Burla, R. Caliendo, M. Camalli, B. Carrozzini, G. L. Cascarano, L. De Caro, C. Giacovazzo, G. Polidori, D. Siliqi, R. Spagna, *J. Appl. Cryst.* **2007**, *40*, 609-613.
3. G. M. Sheldrick, *Acta Cryst.* **2008**, *A64*, 112-122.
4. A. L. Spek, *Acta Cryst.* **2009**, *D65*, 148-155.

2. Syntheses and Characterization Data



Scheme S1. Synthetic procedures of the zinc chlorophyll derivatives with phenylpyridine. (a) acetone, reflux with Soxlet apparatus, 10 days. (b) MeOH, H₂SO₄, overnight. (c) 2,4,6-trimethylpyridine, reflux, 3 h. (d) OsO₄, NaIO₄, AcOH, H₂O, THF, overnight. (e) Bestmann-Ohira reagent, CsCO₃, MeOH, THF, 3 h. (f) bromophenylpyridine, Pd₂(dba)₃, P(*o*-tolyl)₃, Et₃N, toluene, reflux, 24 h. (g) Zn(OAc)₂•2H₂O, MeOH, CHCl₃, 3 h.

Sonogashira Coupling. To a degassed solution of ethynylchlorophyll (100 mg, 0.186 mmol) and bromophenylpyridine (89 mg, 0.38 mmol) in toluene (60 mL) and Et₃N (12 mL) were added P(*o*-tolyl)₃ (66 mg, 0.22 mmol), Pd₂(dba)₃ (26 mg, 0.028 mmol). The mixture was then refluxed for 24 h. After cooling to r.t., the solvent was eliminated in *vacuo* to give a black solid. The crude mixture was purified by column chromatography to afford the product as a brown solid.

Fb3Py: Yield: 41%. ¹H-NMR (CDCl₃): δ / ppm = 9.60 (s, 1H, meso), 9.54 (s, 1H, meso), 9.00 (d, *J* = 1.4 Hz, 1H, Py), 8.68 (dd, *J* = 1.4, 5.5 Hz, 1H, Py), 8.61 (s, 1H, meso), 8.03 (d, *J* = 8.3 Hz, 2H, Ph), 8.01 (dd, *J* = 1.4, 5.5 Hz, 1H, Py), 7.79 (d, *J* = 8.3 Hz, 2H, Ph), 7.46 (m, 1H, Py), 5.30 (d, *J* = 20.2 Hz, 1H, 13²), 5.14 (d, *J* = 20.2 Hz, 1H, 13²), 4.52 (m, 1H, 18-H), 4.22 (m, 1H, 17-H), 3.71 (quartet, *J* = 7.8 Hz, 2H, 8-CH₂CH₃), 3.69, 3.62, 3.55, 3.30 (each s, each 3H, ring CH₃×3, COOMe), 2.76–2.68, 2.62–2.54, 2.35–2.26 (each m, 1H, 1H, 2H, 17¹, 17²), 1.84 (d, *J* = 7.3 Hz, 3H, 18-CH₃), 1.71 (t, *J* = 7.8 Hz, 3H, 8-CH₂CH₃), 0.30 (bs, 1H, NH), and -1.84 (bs, 1H, NH); APCI-HRMS: calcd for C₄₅H₄₁N₅O₃, MH⁺, 700.3288, found 700.3291; GPC: *V*_R = 163.4 mL (100%).

Fb4Py: Yield: 75%. ¹H-NMR (CDCl₃): δ / ppm = 9.60 (s, 1H, meso), 9.52 (s, 1H, meso), 8.75 (d, *J* = 6.0 Hz, 2H, Py), 8.61 (s, 1H, meso), 8.02 (d, *J* = 8.5 Hz, 2H, Ph), 7.83 (d, *J* = 8.5 Hz, 2H, Ph), 7.63 (d, *J* = 6.0 Hz, 2H, Py), 5.29 (d, *J* = 19.7 Hz, 1H, 13²), 5.14 (d, *J* = 19.7 Hz, 1H, 13²), 4.52 (m, 1H, 18-H), 4.33 (m, 1H, 17-H), 3.70 (quartet, *J* = 7.8 Hz, 2H, 8-CH₂CH₃), 3.68, 3.62, 3.54, 3.28 (each s, each 3H, CH₃×3, COOMe), 2.76–2.67, 2.63–2.55, 2.36–2.26 (each m, 1H, 1H, 2H, 17¹, 17²), 1.84 (d, *J* = 7.3 Hz, 3H, 18-CH₃), 1.71 (t, *J* = 7.8 Hz, 3H, 8-CH₂CH₃), 0.26 (bs, 1H, NH), and

-1.87 (bs, 1H, NH); APCI-HRMS: calcd for C₄₅H₄₁N₅O₃, MH⁺, 700.3288, found 700.3273; GPC : V_R = 167.6 mL (100%).

Zinc Insertion. To a solution of the free-base compounds (50 mg, 0.07 mmol) in CHCl₃ (56 mL) was added sat. Zn(OAc)₂•2H₂O in MeOH (5 mL). After stirring for 3 h, 4% NaHCO₃ was added. The organic layer was separated, and was washed with H₂O. The solvent was eliminated in *vacuo* to quantitatively give the product as a green solid.

Zn3Py: ¹H-NMR (CDCl₃): δ/ppm = 9.61 (s, 1H, meso), 9.56 (s, 1H, meso), 8.40 (s, 1H, meso), 7.82 (d, J = 7.3 Hz, 2H, Ph), 6.92 (d, J = 5.5 Hz, 1H, Py), 6.68 (d, J = 7.3 Hz, 2H, Ph), 5.97 (bt, J = 6.0 Hz, 1H, Py), 5.34 (d, J = 19.2 Hz, 1H, 13²), 5.19 (d, J = 19.2 Hz, 1H, 13²), 4.43 (m, 1H, 18-H), 4.30 (m, 1H, 17-H), 3.74 (m, 2H, Py, 3-CH₂CH₃), 3.74, 3.63, 3.51, 3.30 (each s, each 3H, ring CH₃×3, COOMe), 3.30 (bs, 1H, Py), 2.72–2.64, 2.54–2.46, 2.38–2.29, 2.24–2.16 (each m, each 1H, 17¹, 17²), and 1.76–1.69 (m, 6H, 8-CH₂CH₃, 18-CH₃); APCI-HRMS: calcd for C₄₅H₄₀N₅O₃Zn, MH⁺, 762.2423, found 762.2414.

Zn4Py: ¹H-NMR (CDCl₃): δ/ppm = 9.59 (s, 1H, meso), 9.36 (s, 1H, meso), 8.39 (s, 1H, meso), 7.60 (d, J = 8.0 Hz, 2H, Ph), 6.97 (d, J = 8.0 Hz, 2H, Ph), 6.17 (bs, 2H, Py), 5.19 (d, J = 19.7 Hz, 1H, 13²), 5.07 (d, J = 19.7 Hz, 1H, 13²), 4.44 (m, 1H, 18-H), 4.25 (m, 1H, 17-H), 3.85 (bs, 2H, Py), 3.74 (quartet, J = 7.3 Hz, 2H, 8-CH₂CH₃), 3.70, 3.53, 3.38, 3.19 (each s, each 3H, ring CH₃×3, COOMe), 2.63–2.58, 2.43–2.38, 2.36–2.26, 2.08–2.00 (each m, each 1H, 17¹, 17²), 7.3 (d, J = 7.3 Hz, 3H, 18-CH₃), and 1.70 (t, J = 7.3 Hz, 3H, 8-CH₂CH₃); APCI-HRMS: calcd for C₄₅H₄₀N₅O₃Zn, MH⁺, 762.2423, found 762.2400.

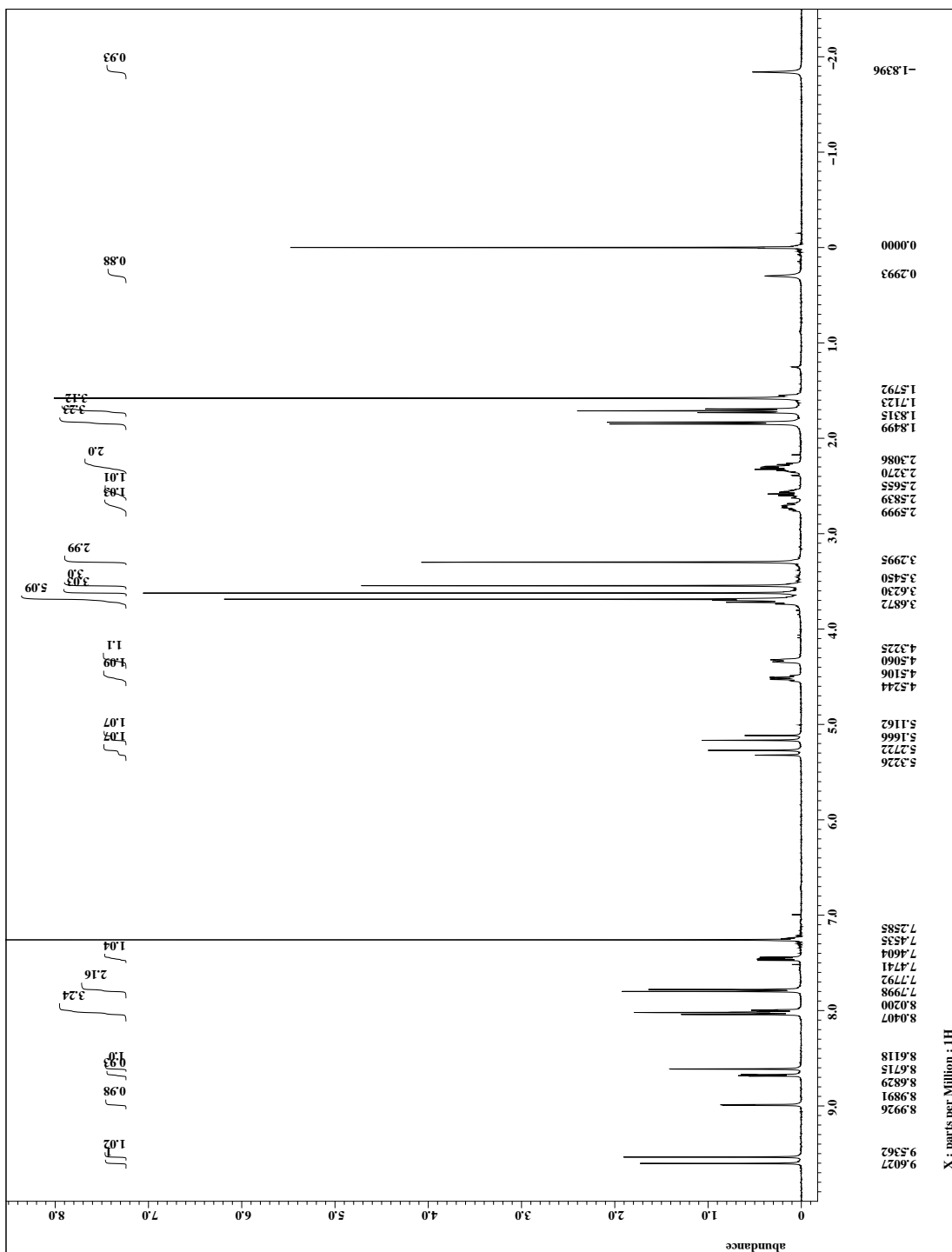


Figure S1. $^1\text{H-NMR}$ spectrum of Fb3Py.

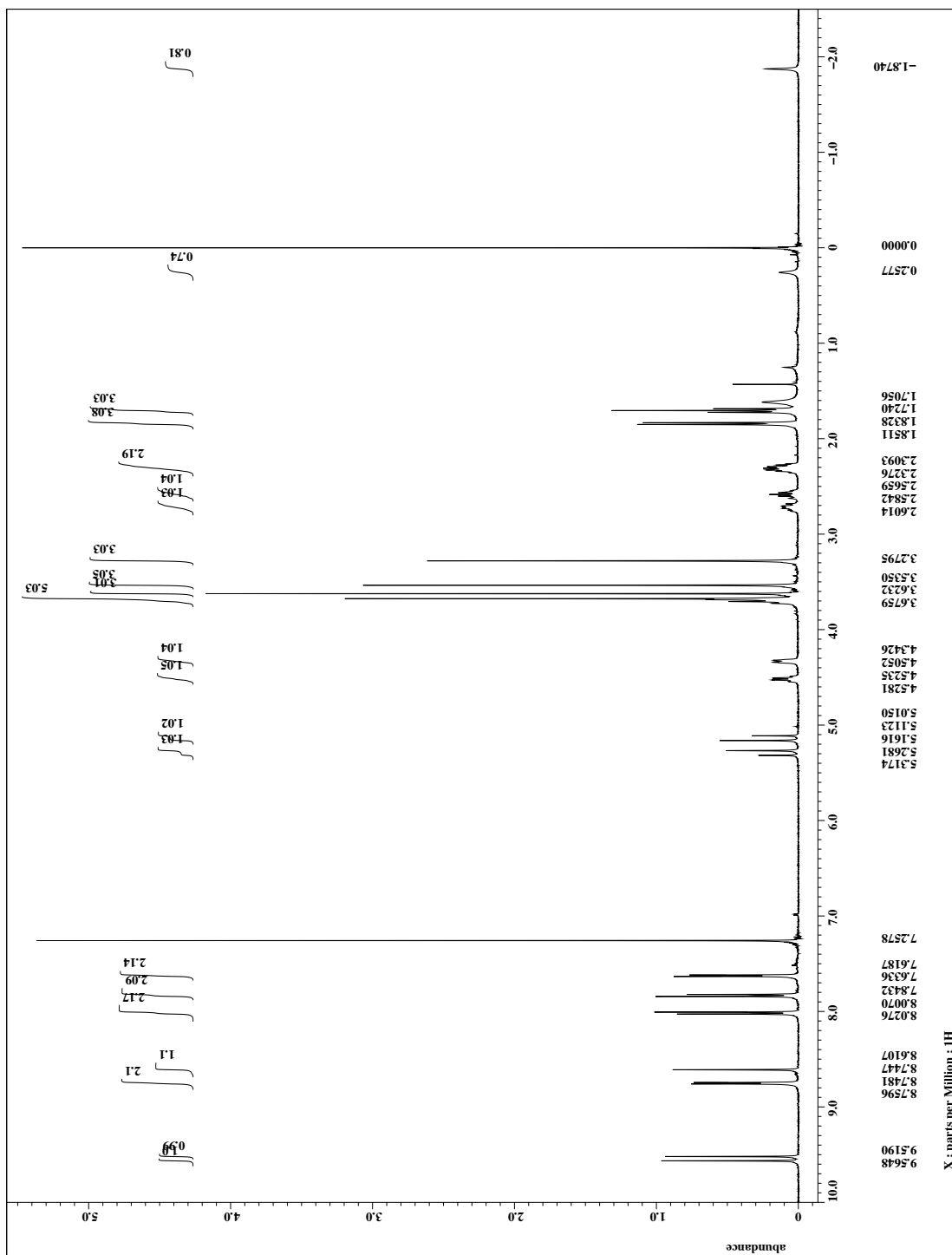


Figure S2. $^1\text{H-NMR}$ spectrum of Fb4Py.

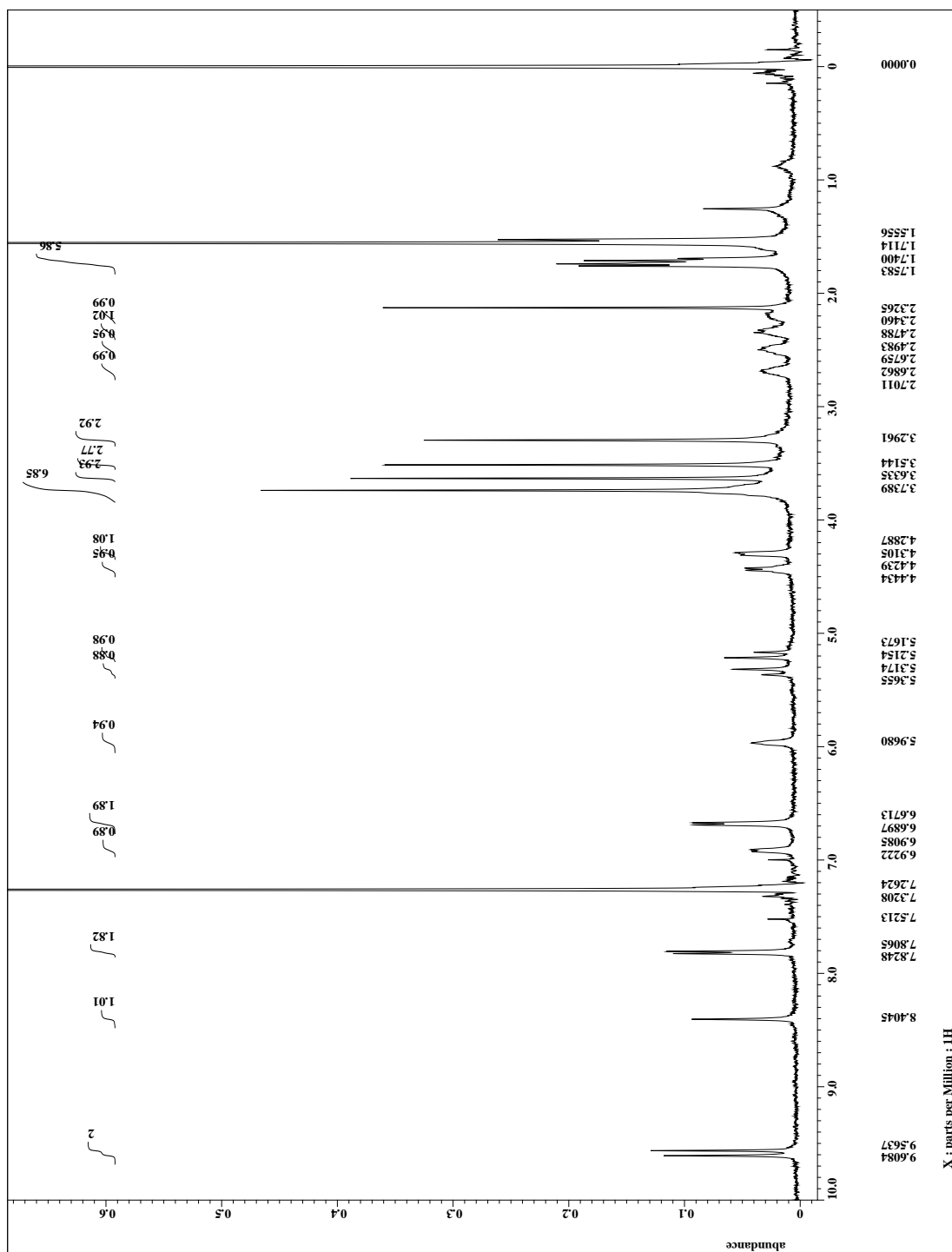


Figure 3. $^1\text{H-NMR}$ spectrum of Zn_3Py .

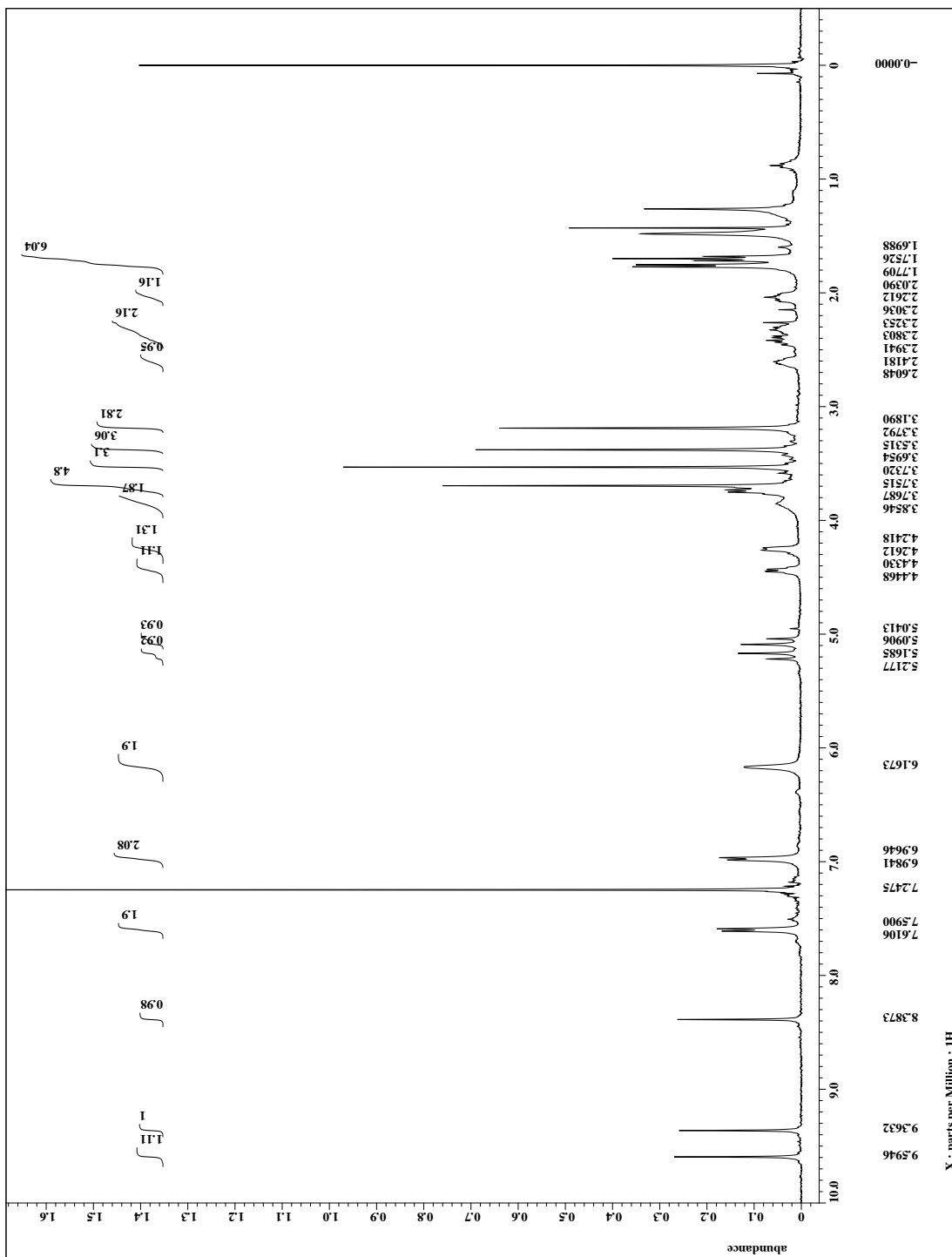


Figure S4. $^1\text{H-NMR}$ spectrum of Zn4Py.

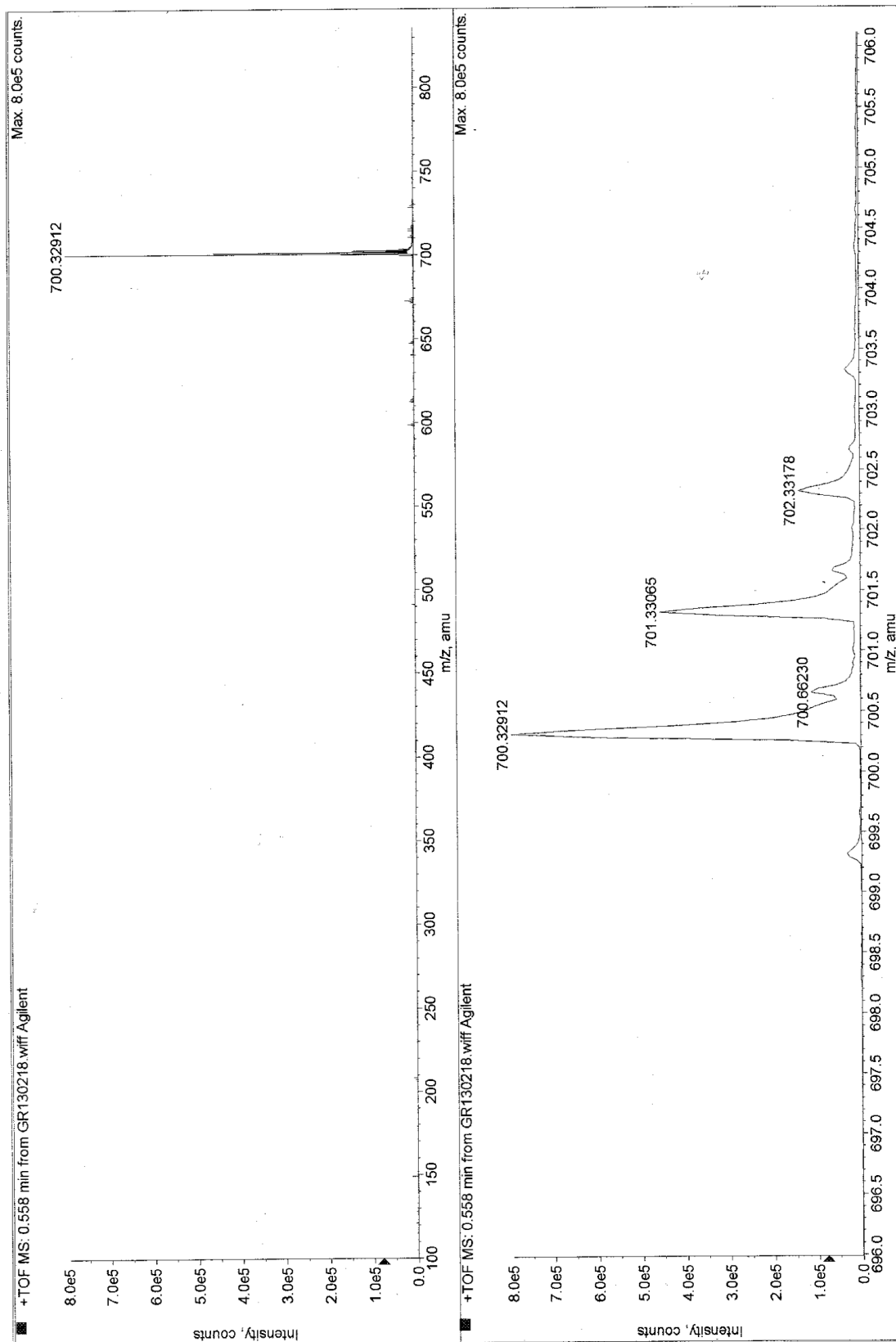


Figure S5. APCI-HRMS spectrum of Fb3Py.

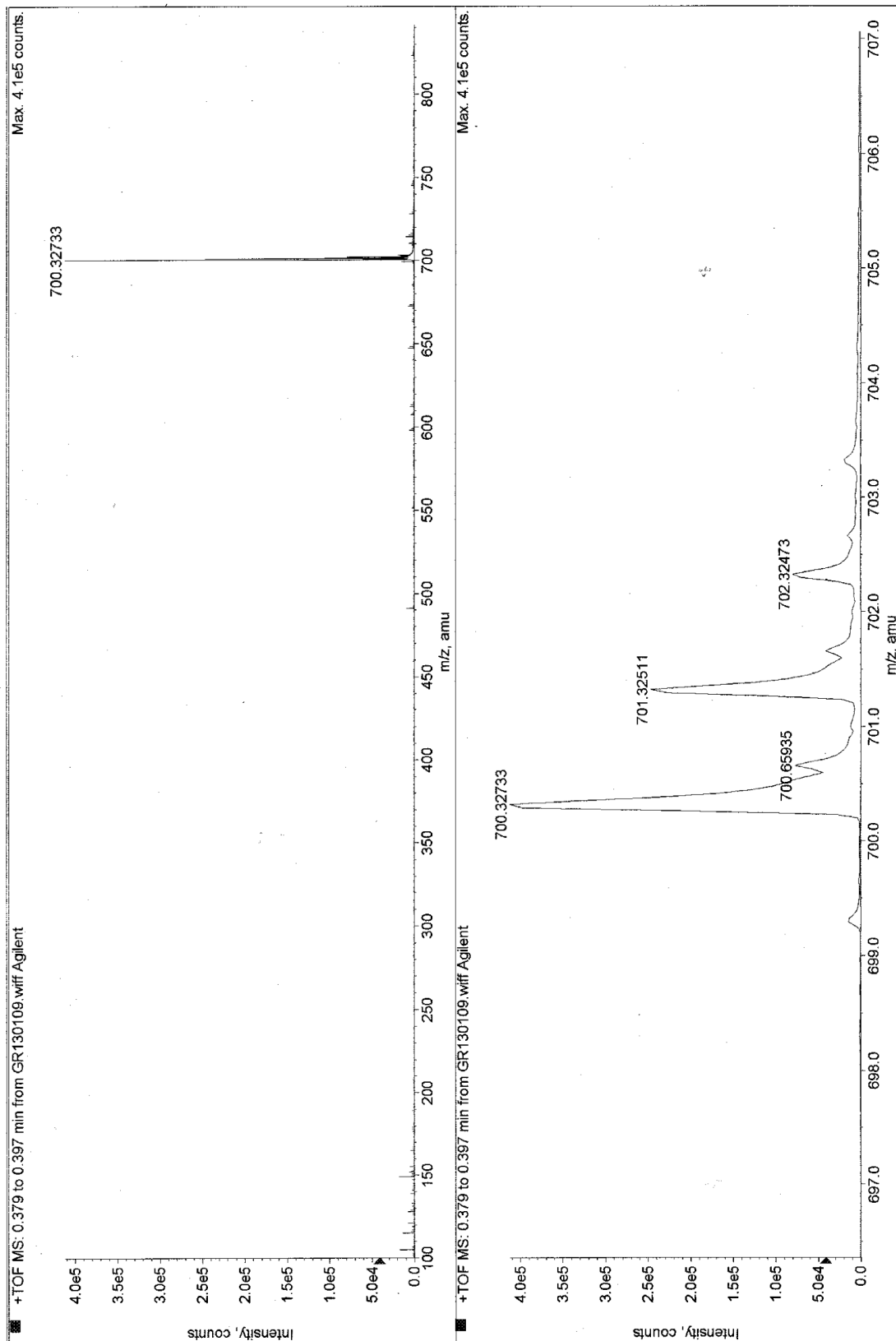


Figure S6. APCI-HRMS spectrum of Fb4Py.

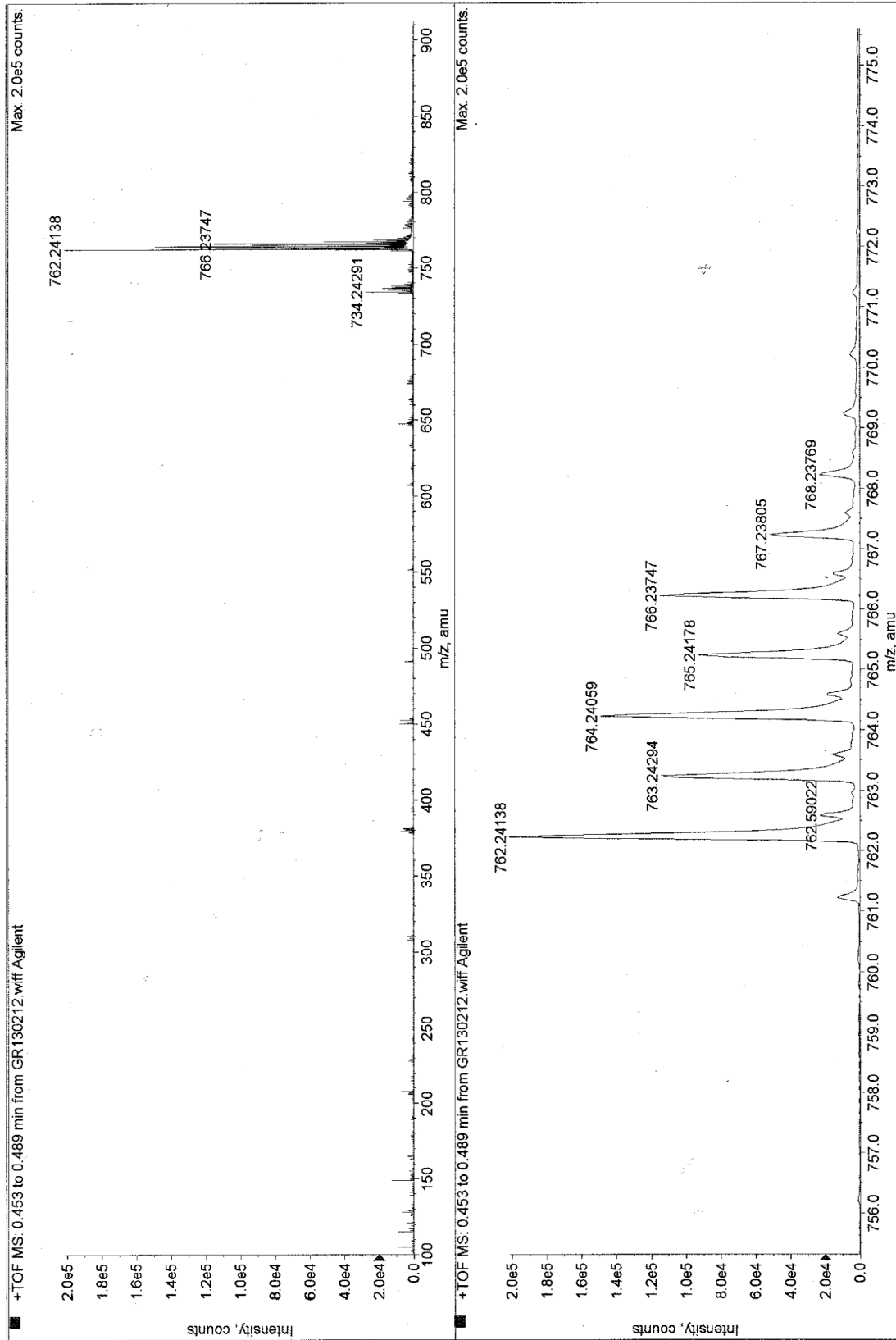


Figure S7. APCI-HRMS spectrum of Zn₃Py.

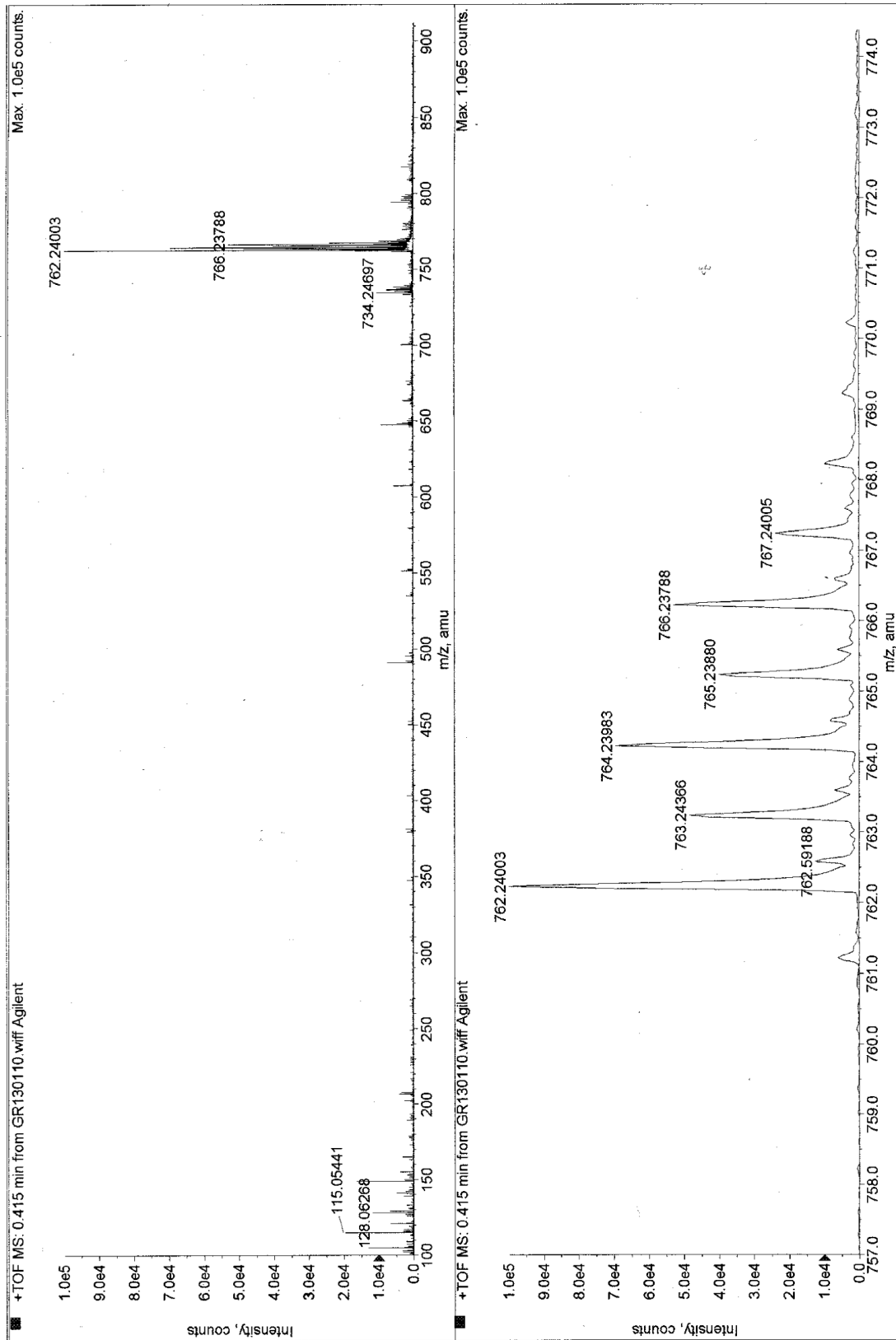


Figure S8. APCI-HRMS spectrum of Zn₄Py.

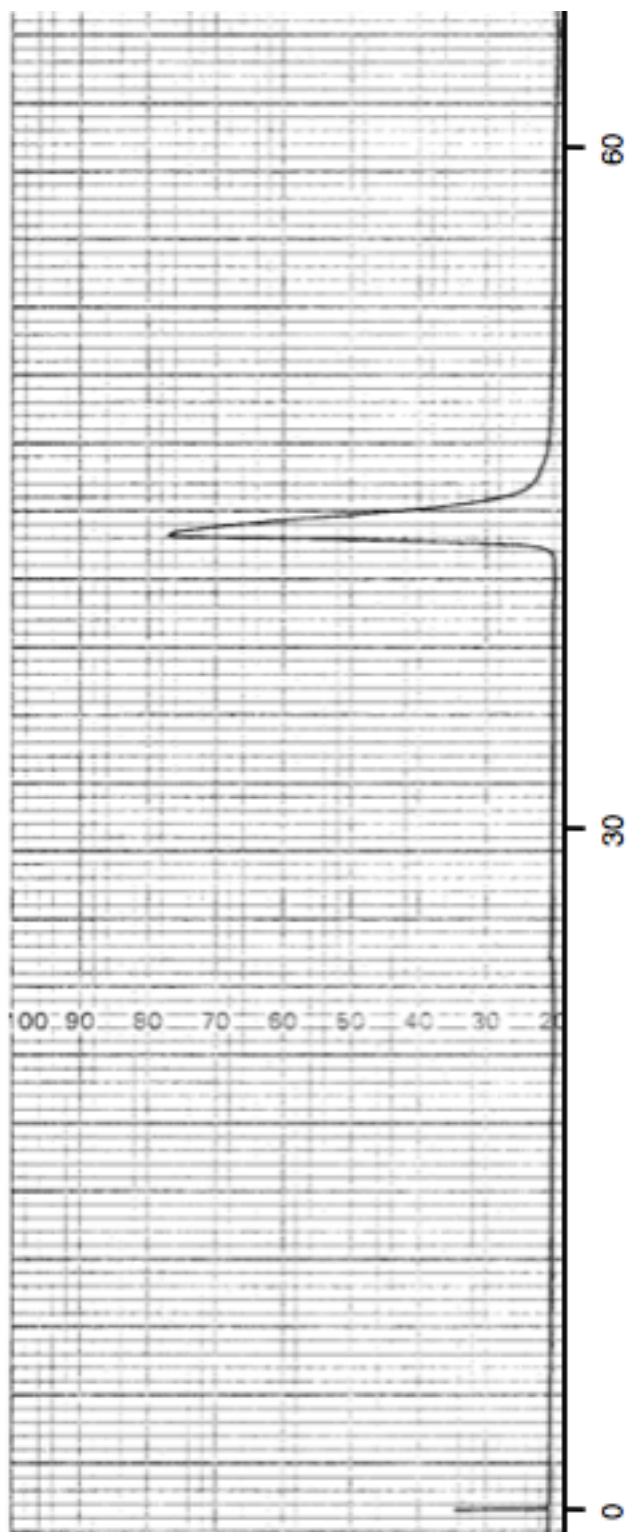


Figure S9. GPC chromatogram of Fb3Py.

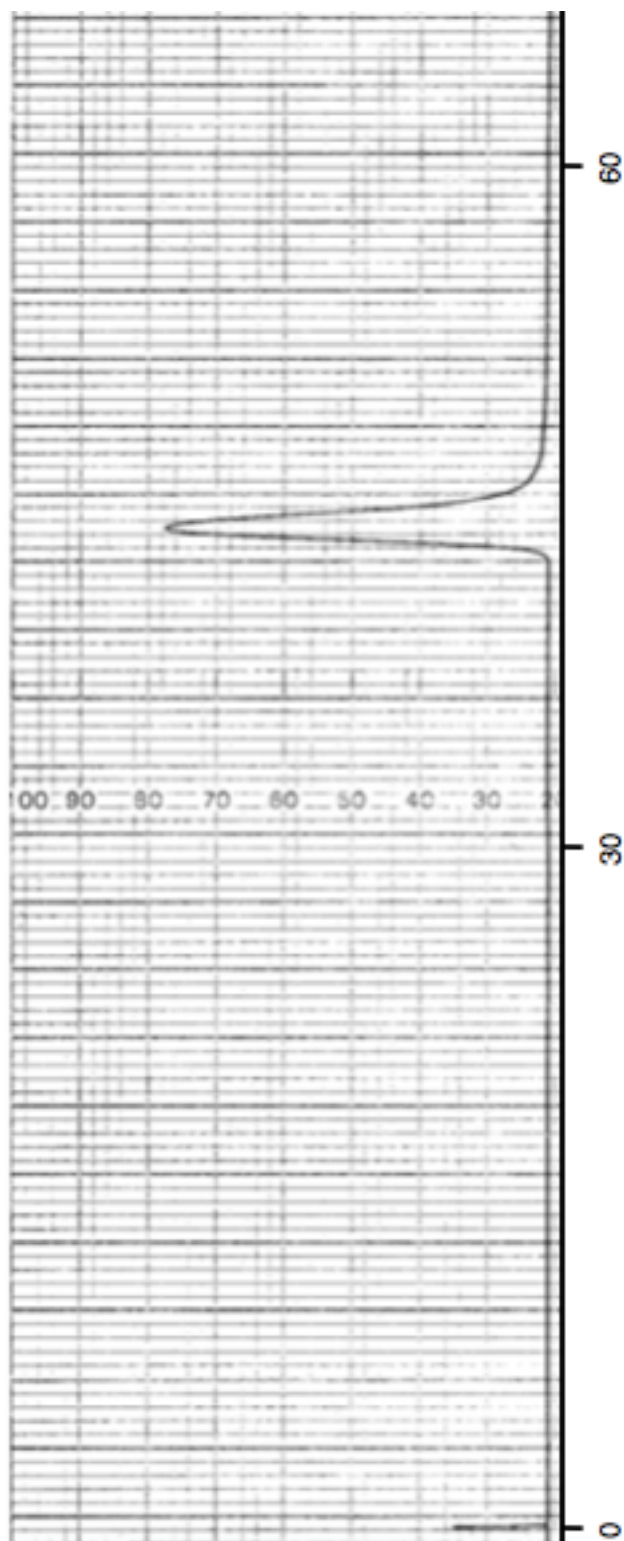


Figure S10. GPC chromatogram of **Fb4Py**.

3. Comparison of $^1\text{H-NMR}$ Spectra for the Free-Base Derivatives and Their Zinc Complexes

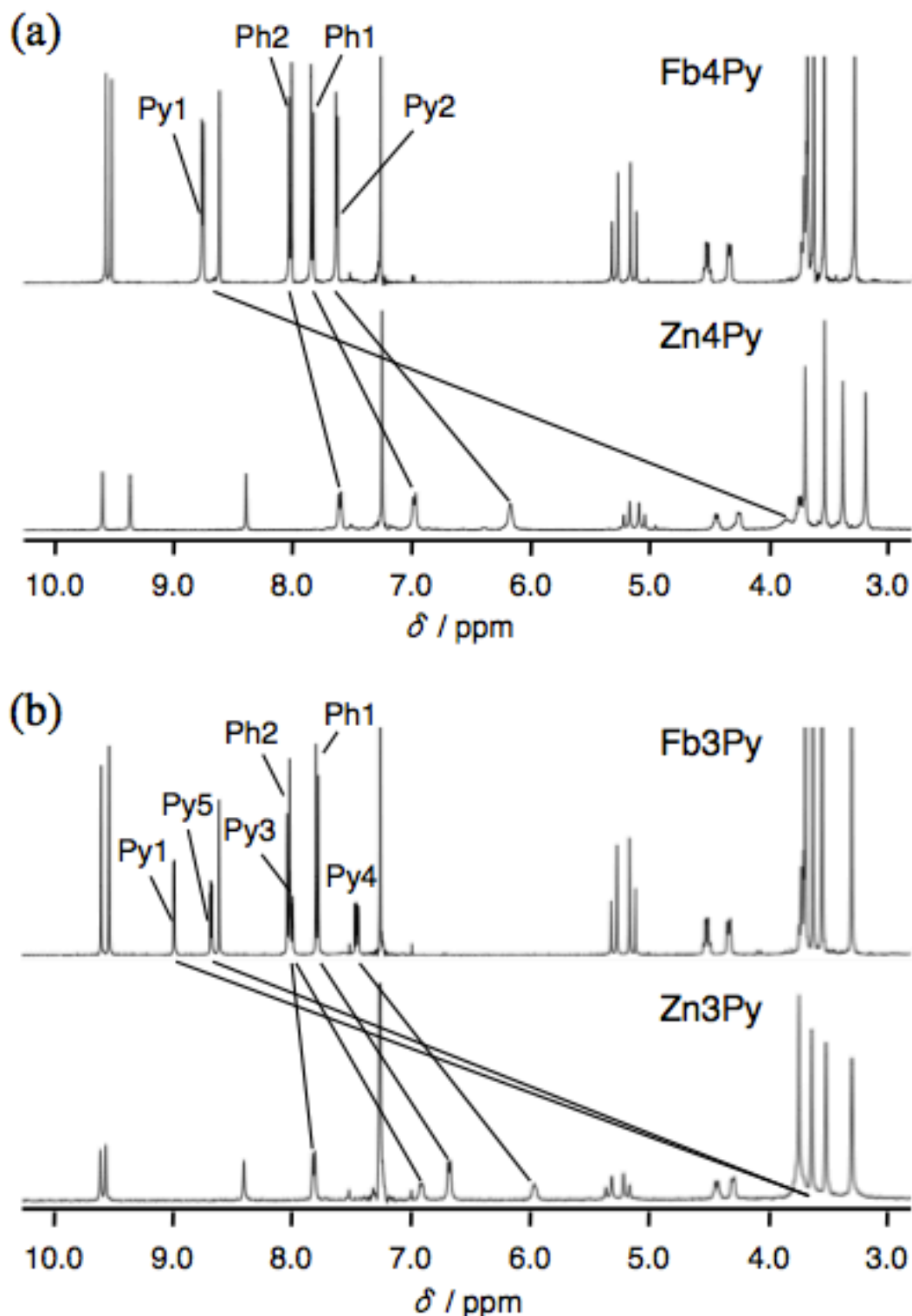


Figure S11. $^1\text{H-NMR}$ spectra of (a) **Fb4Py** and **Zn4Py**, (b) **Fb3Py** and **Zn3Py** in CDCl_3 at 298 K (ca 10 mM for free-base compounds, saturated solution for zinc complexes due to poor solubility). The solid lines indicate the upfield shift upon zinc insertion. See Chart1 for proton labels.

4. Crystallographic Data

Table S1. Crystallographic Data for **Zn3Py**.

Compound	Zn3Py
Empirical formula	C ₁₀₂ H ₁₀₆ N ₁₀ O ₉ Zn ₂
Formula weight	1746.70
Color, Habit	Black, Rhombic
Temperature / K	93
Wavelength / Å	0.71075
Crystal system	Monoclinic
Space group	<i>P</i> 2 ₁
Unit cell dimensions / Å	<i>a</i> = 14.904(4) <i>b</i> = 14.159(3) <i>c</i> = 21.949(5)
Volume / Å ³	4563.1(19)
Z	2
Absorption coefficient / mm ⁻¹	0.589
F(000)	1840
Crystal size / mm ³	0.25×0.16×0.13
θ for data collection	3.0 to 27.5
Index ranges	$-17 \leq h \leq 19$, $-18 \leq k \leq 18$, $-24 \leq l \leq 27$
Reflections collected	37583
Independent reflections	19583
Completeness	97.5% ($\theta = 27.48^\circ$)
Absorption correction	Numerical
Max. and min. transmission	0.926 and 0.888
Refinement method	Full-matrix least-squares on F^2
Flack parameter	0.061(11)
Data/restraints/parameters	19583/341/999
Goodness-of-fit on F^2	1.021
Final <i>R</i> indices [$I > 2\sigma(I)$]	$R_1 = 0.0787$
<i>R</i> indices (all data)	$wR_2 = 0.2032$
Largest diff. peak and hole / e Å ⁻³	1.066 and -0.811

Table S2. Crystallographic Data for **Zn4Py**.

Compound	Zn4Py
Empirical formula	$C_{45}H_{39}N_5O_3Zn$
Formula weight	763.18
Color, Habit	Black, Needle
Temperature / K	93
Wavelength / Å	0.71075
Crystal system	Monoclinic
Space group	$P2_1$
Unit cell dimensions / Å	$a = 10.372(7)$ $b = 22.684(14)$ $c = 18.375(11)$
Volume / Å ³	4187.(5)
Z	4
Absorption coefficient / mm ⁻¹	0.630
F(000)	1592
Crystal size / mm ³	0.34×0.050×0.020
θ for data collection	2.10 to 25.30
Index ranges	$-12 \leq h \leq 12, -27 \leq k \leq 27, -22 \leq l \leq 21$
Reflections collected	29029
Independent reflections	14538
Completeness	92.4% ($\theta = 25.26^\circ$)
Absorption correction	multi-scan
Refinement method	Full-matrix least-squares on F^2
Flack parameter	0.10(2)
Data/restraints/parameters	14538/333/968
Goodness-of-fit on F^2	1.046
Final R indices [$I > 2\sigma(I)$]	$R_1 = 0.1136$
R indices (all data)	$wR_2 = 0.2384$
Largest diff. peak and hole / e Å ⁻³	0.803 and -0.528

Table S3. Selected Structural Parameters for **Zn3Py** Molecules

	Red		Blue
		Angle / °	
$\angle N_1-Zn-N_2$	91.3(3)		91.6(3)
$\angle N_2-Zn-N_3$	88.0(3)		87.1(3)
$\angle N_3-Zn-N_4$	87.9(3)		89.4(3)
$\angle N_4-Zn-N_1$	88.9(3)		88.4(3)
		Distance / Å	
N_1-Zn	2.033(6)		1.995(6)
N_2-Zn	2.072(8)		2.056(9)
N_3-Zn	2.012(6)		1.992(6)
N_4-Zn	2.186(9)		2.210(7)
$N_{py}-Zn$	2.179(7)		2.161(7)
$N_1N_2N_3N_4-Zn$	0.272		0.258

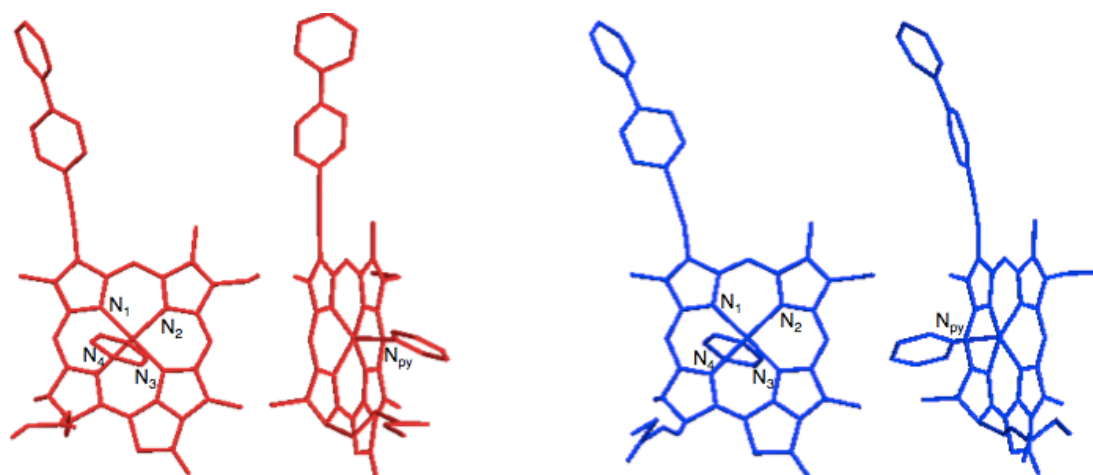
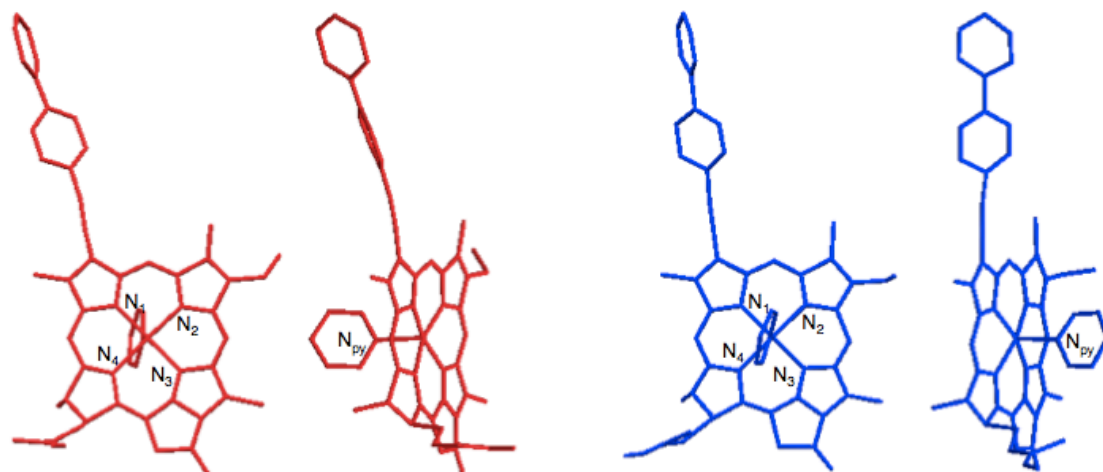


Table S4. Selected Structural Parameters for **Zn4Py** Molecules

	Red	Blue
		Angle / °
$\angle N_1-Zn-N_2$	90.5(6)	91.2(6)
$\angle N_2-Zn-N_3$	87.6(7)	86.7(6)
$\angle N_3-Zn-N_4$	88.3(7)	89.3(6)
$\angle N_4-Zn-N_1$	89.5(6)	88.6(6)
		Distance / Å
N_1-Zn	2.04(1)	2.00(1)
N_2-Zn	2.10(2)	2.05(1)
N_3-Zn	2.02(2)	2.02(2)
N_4-Zn	2.16(2)	2.19(1)
$N_{py}-Zn$	2.13(2)	2.15(2)
$N_1N_2N_3N_4-Zn$	0.279	0.277



5. Relative Efficiency of Förster-type Energy Transfer

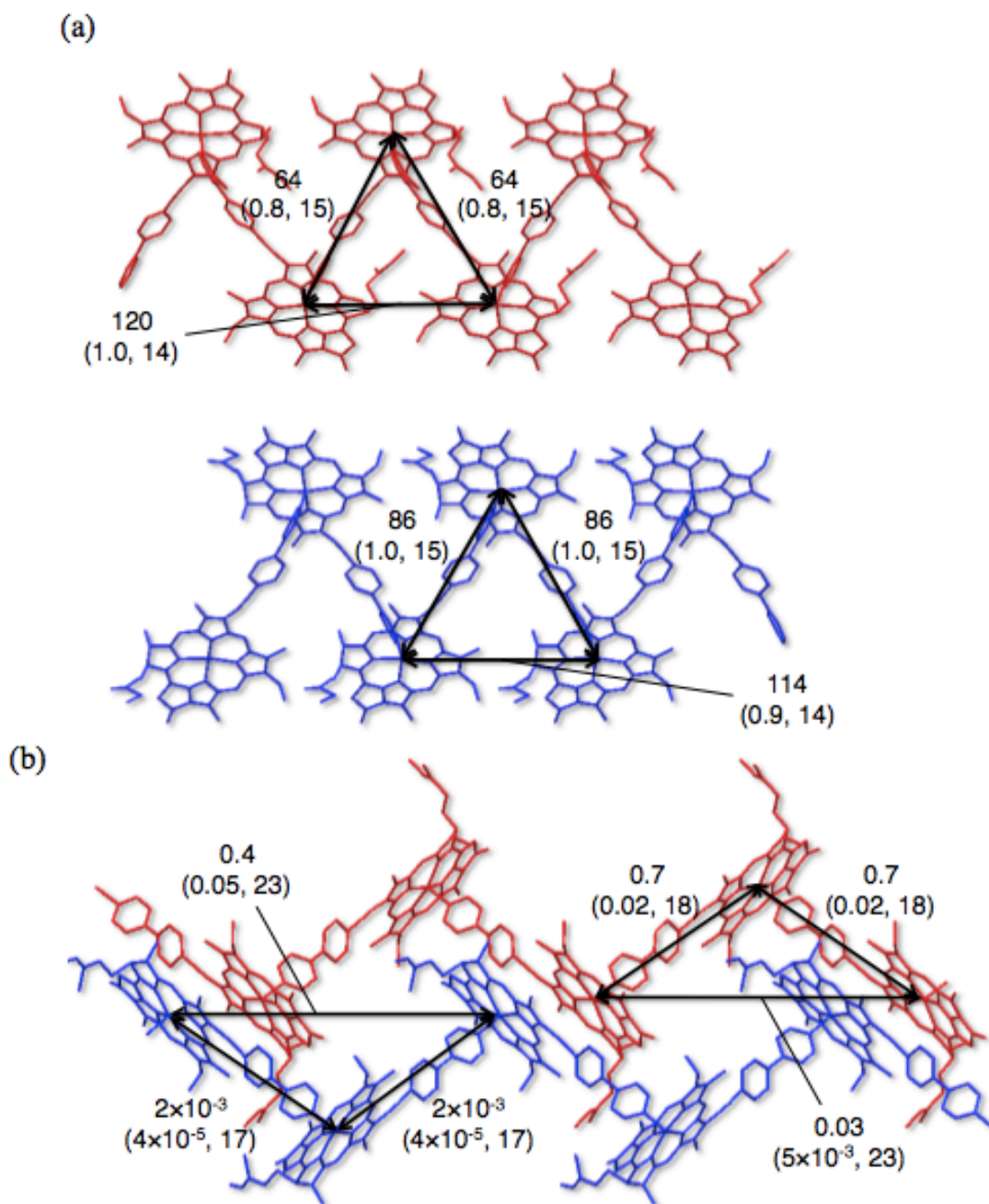


Figure S12. Values of $(k^2/r^6 \times 10^9)$ (in \AA^{-6}) as a measure of relative efficiencies of Förster-type energy transfer in the coordination polymers of (a) **Zn3Py** and (b) **Zn4Py**. The arrows represent the pair of donor and acceptor molecules. The orientation factor k^2 and the distance r (in \AA) are shown in parenthesis.

6. Fluorescence Spectra

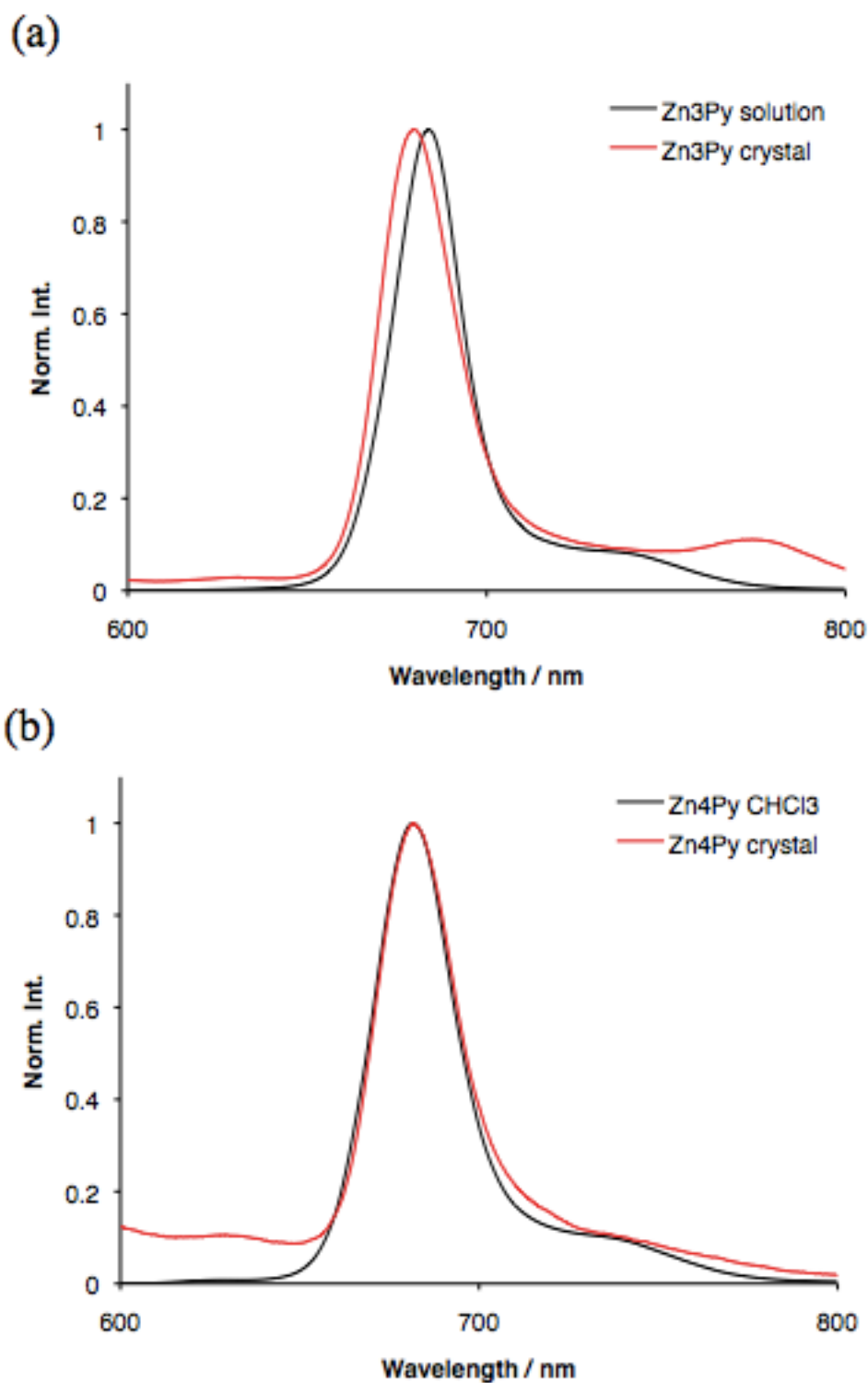


Figure S13. Fluorescence spectra of (a) **Zn3Py** ($\lambda_{\text{ex}} = 439$ nm) and (b) **Zn4Py** ($\lambda_{\text{ex}} = 432$ nm) in CHCl_3 (ca. $10 \mu\text{M}$) and their crystals. The spectra of the crystals were measured in liquid paraffin by a reflection geometry.